Chapter 23
Quad-Rotorcraft to Harness High-Altitude Wind Energy

Bryan W. Roberts

Abstract Wind at higher altitudes is generally stronger and more persistent than near-surface wind. At many locations the atmospheric flows have annual average power densities that by far exceed these of any other renewable energy sources. Capturing this energy potential has been the objective of a pioneering airborne wind energy concept based on a tethered rotorcraft which was invented in Australia in the 1980s. The chapter summarizes early research with a towed generating rotor, wind tunnel tests and a low-altitude atmospheric test vehicle. These tests have confirmed the feasibility of kite-like flight of a craft having twin or quadruple rotors with the rotors simultaneously generating electricity. Using high-altitude wind data statistics for Australia and the USA it is shown that near base-load electrical outputs can be achieved at capacity factors of 70 to 80%. The governing physical relations of the technology are derived from classical helicopter theory leading to the rotor thrusts and the rotors' limits to power generation. The range of useful tip-speed ratios is presented for the complete range of rotor disk incidence angles. This mathematical model is used to describe the low-altitude operation of a small quad-rotorcraft. The model is suitable to predict the performance of a multi-megawatt machine. The final contribution of the chapter is a dynamic analysis of the system to devise a control strategy for the craft's power output, pitch, roll and yaw, using purely blade collective pitch action.

23.1 Introduction

It is proposed that a tethered quad-rotorcraft can harness the enormously powerful winds at higher altitude, thereby generate electricity from these winds [3]. It is well known that two major jet streams exist in each Earth hemisphere at higher altitudes.

Bryan W. Roberts (✉)
Altitude Energy Pty. Ltd., Australia
e-mail: trytables@bigpond.com

These streams are called the sub-tropical jet and the polar-front jet. The former are of particular relevance as they exist in bands approximately 1000 km wide over the Mediterranean, Northern India, China, Southern Japan, North America, Africa, Australia, South America and elsewhere. These streams have enormous energy and persistence compared to near-surface winds. They are formed by sunlight falling on the tropics in combination with the Earth's rotation. The formation of these jet streams can be seen in Fig. 23.1, which is a section through the Earth showing how heated air rises in the tropics (0° latitude) and then moves towards the North and South poles (90° latitude) after it rises to tropopause altitude. Subsequently at

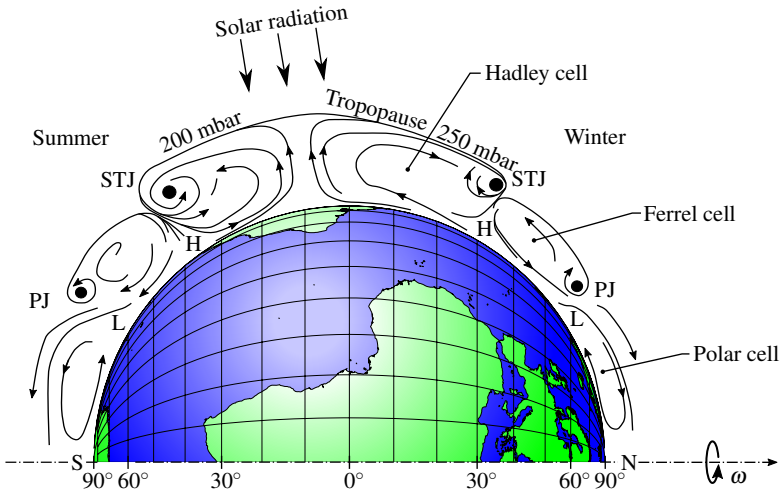

Fig. 23.1 Global atmospheric flow mechanisms and formation of jet streams (STJ: subtropical jet, PJ: polar jet, H: high pressure region, L: low pressure region). Thickness of atmosphere not to scale

increasing latitudes, due to the Coriolis acceleration, the air moves from west to east to form the jet streams.

Furthermore, compared to ground-based turbines operating in low-velocity winds at the bottom of the Earth's boundary layer, these jet stream winds offer a potential annual energy output of about two orders of magnitude greater than that obtainable from ground-based turbines of equivalent rotor area.

The following Sect. 23.2 presents two resource studies comprising wind data for near-surface altitudes up to the tropopause level, where the jets generally reside. Section 23.3 outlines several harvesting systems based on the tethered rotorcraft principle. Section 23.4 describes a wind tunnel analysis of a small-scale model while Sect. 23.5 provides details on the design and testing of an outdoors rotorcraft. In Sects. 23.6 to 23.9 the quad-rotorcraft configuration is analyzed in detail, discussing important aspects of its operation. Section 23.10 describes the stability and control and Sect. 23.11 concludes the chapter. The preliminary content of the present chapter has been presented at the Airborne Wind Energy Conference 2015 [12].

23.2 Upper Wind Data for Australia and USA

The southern and northern sub-tropical jet streams (around 30 to 40° latitude) cross the planet in a W-E direction. The jet stream is invariably present, sometimes bifurcated, with annual average velocities of around 130 km/h. The passage of the jet is observed to meander north and south so that any fixed land or ocean site is swept by the jet. Extensive studies of the wind statistics have been undertaken by Atkinson et al [1] for Australia and O'Doherty and Roberts [10] for the USA. In Australia an annual average wind power density of 19 kW/m^2 is achievable, while in the USA the maximum annual average power density is 17 kW/m^2. It might be argued that the generally higher power densities in the southern hemisphere are due to a colder pole in the south relative to that in the north.

Figure 23.2 shows the isopleths of annual average power density over Australia at an altitude of 250 mbar. It may be seen therein that the power distribution is

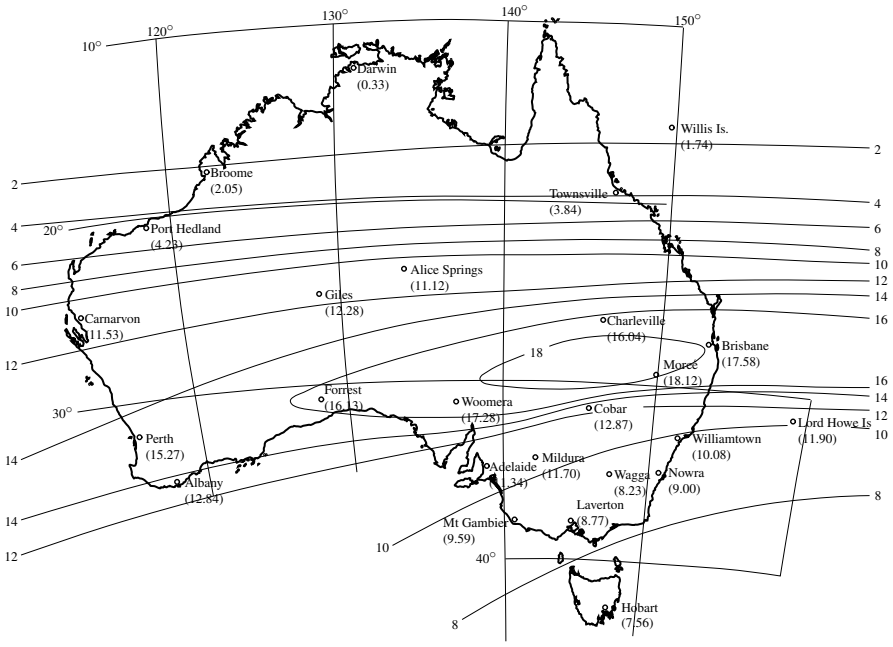

Fig. 23.2 Isopleths of the annual average power density P_w [kW/m^2] over Australia at an altitude of 250 mbar which corresponds to 10 km altitude

spatially well organized because of the lack of high mountains tending to upset the orderly flow of air.

A similar graph for USA is not so well organized [10], possibly due to the presence of the Rocky Mountains. A standard wind energy technique is to represent the cumulative probability distribution $F(v_w)$ of wind speed v_w by a Weibull model

$$F(v_{\mathrm{w}}) = 1 - \exp\left[-\left(\frac{v_{\mathrm{w}}}{v_{\mathrm{w},0}}\right)^{n}\right], \quad \text{for} \quad v_{\mathrm{w}} > 0, \tag{23.1}$$

where $v_{\mathrm{w},0}$ and n are two constants chosen to give a good fit to the observed data.

Figure 23.3 shows the cumulative probability distribution for Albany, NY, USA. It is typical of the US states in that general area. Because special "Weibull paper" is

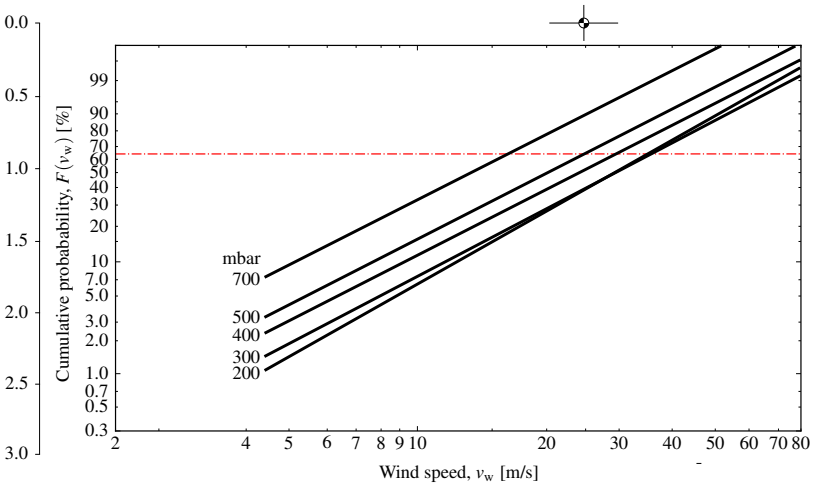

Fig. 23.3 Annual probability distribution of velocity in Albany, NY, USA [10]

used the cumulative probability distributions of the wind speed are straight lines. A sample use of the diagram is as follows. At an altitude of 300 mbar wind speeds of 10 m/s or lower will occur for approximately 7% of the time, namely 613 hours per annum. This period per annum below the so called threshold velocity of 10 m/s is made-up by the number of down-times per annum multiplied by the average down-time in each event. An average down-time is about 24 hours. Furthermore, it is shown in references [1] and [10], the latter providing details for some 50 sites across the USA, that the winds are generally stronger in winter than in summer. The data given in Fig. 23.3 is for one of the best sites in the USA and it is almost identical, although a little less optimal, than the best site in Australia, around Moree in the state of North South Wales.

The average annual power densities quoted above are the highest power densities on Earth for any large-scale renewable resource. These power densities vastly exceed that of solar radiation. The latter is generally around 0.25 kW/m^2 at the surface depending on latitude. Furthermore, high-altitude wind exceeds the power density of any other renewable energy resource found on Earth. They exceed the resource of near surface winds, that of ocean currents, tidal and the geothermal resources.

Hoffert, Caldeira et al. [7] estimate that the total thermal power consumption by human civilization is 10 TW, which is about 1% of the total amount of power

dissipated in the planet's wind system. Most of this planetary wind energy is concentrated in the jet stream system, so that a maximum energy extraction of around 1% would not have any adverse impact on the Earth's environment or climate.

This high-altitude wind resource is just a few kilometers above the surface of the planet, where the energy is needed. Because of its vast power and persistent nature it would, if captured, be a very attractive and inexhaustible power supply.

23.3 Various Capture Systems

One of the earliest suggestions for high-altitude capture was that made by Manalis [9] in 1976. Various systems have been examined since. These range from tethered balloons, tethered fixed-winged craft, tethered kites in simple or crosswind flight, climbing and descending devices and rotorcraft. The preferred option here is a tethered rotorcraft, a variant of the gyroplane principle, where conventional rotors operating at a significant disk incidence generate power in the on-coming wind, while simultaneously producing sufficient lift to keep the system aloft.

In engineering design, if some component performs two important functions simultaneously, then this component should be featured. In the current rotorcraft concept the rotors provide lift while simultaneously generating power. It is this important dual function that is the centerpiece of the current work.

Roberts and Blackler [17] confirmed the power generating characteristics of a rotor at incidence to the wind by mounting a simple, flap-articulate rotor above a test vehicle as seen in Fig. 23.4. By moving the test vehicle through still air they

Fig. 23.4 Test setup for rotor at incident angle

were able to obtain a confirmation of the power generation principle along with an estimate of the accuracy of the theoretical predictions.

The two-bladed ($b = 2$) rotor had a linear twist angle of $\theta_1 = +8^\circ$, while the collective pitch angle was pre-set to $\theta_0 = -8^\circ$ using specially machined blade grips. The rotor's torque output was measured, while the rotor thrust was not recorded because if the torque output was shown to agree with the extended theory of Gessow and Crim [4], then it is highly likely the thrust coefficient would agree since it was derived from a common theory. This avoided the added complication of constructing a thrust measuring and recording system. The results of these experiments are shown in Fig. 23.5. Therein the measured rotor-shaft torque coefficient C_Q is somewhat

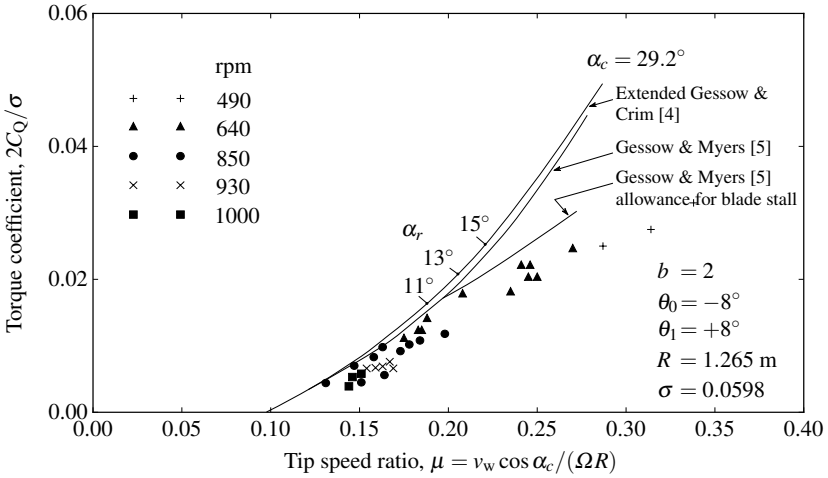

Fig. 23.5 Torque parameter versus tip speed ratio (test date at Schofields: 28 November 1979)

less than the calculated values using accepted profile drag values. Note that the coefficient C_Q used in Fig. 23.5 is in helicopter terminology, namely based on the rotor tip speed ΩR, not the wind speed v_w. Symbols R and Ω denote the radius and angular velocity of the rotor. The parameter $2C_Q/\sigma$ is a conventional helicopter parameter, where σ is the rotor solidity defined as the total blade area divided by the swept area of the rotor. The rotor's control axis angle is $\alpha_c = 29.2^\circ$ and three specific values $\alpha_r = 11, 13$ and 15° are the angle of attack values on the retreating blade at a standard reference location on the blade's span as defined in the helicopter texts such as Gessow and Myers [5]. This technique is used in helicopter work to set limits on rotor operation without having excessive retreating blade stall. A limit of 13° has been used throughout the current work.

However, the results agree well when allowance is made for increased aerodynamic drag at the test Reynolds number. The conventional method of allowing for increased profile drag due to retreating blade stall is also demonstrated by the test

results. The small angle theory of Gessow and Myers [5] can be seen to correspond with the extended theory of Gessow and Crim [4].

Encouraged by the results of Fig. 23.5 it was decided to construct a wind-tunnel model of a twin, side-by-side rotorcraft to explore the handling in a conversion of the craft from helicopter to generate mode and vice versa, while in-flight.

23.4 Wind Tunnel Model

A wind-tunnel model was constructed as described in detail in reference [17]. The model had twin, contra-rotating rotors, with $R = 0.335$ m and $\sigma = 0.0462$ and is shown in Fig. 23.6. The airflow in the side view is from right to left and the twin

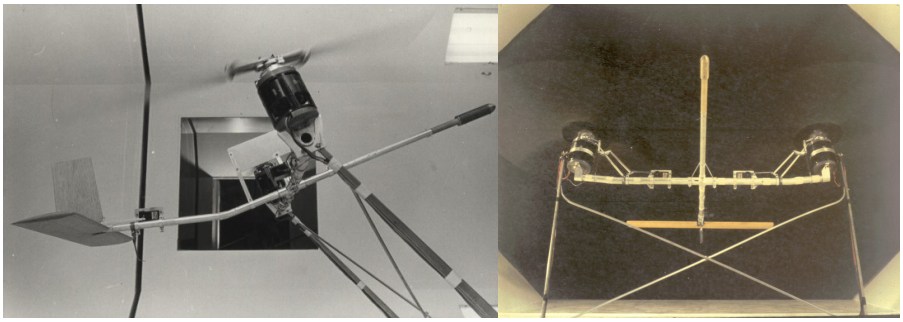

Fig. 23.6 Wind tunnel model in side view (left) and front view (right) in generating mode

rotors are driven by two separate, permanent-magnet DC motor/generators.

Because of a slight mismatch in the manually controlled rotational speed the closely spaced tips tended to interact and induce vibration. Therefore a thin vertical, edge-on partition was used to aerodynamically isolate the rotor tips. A horizontal tailplane was used for longitudinal stability and control, while the tethering arrangement was a twin-bar frame hinged under the rotors and at the tunnel floor. This frame was cross-braced to effectively eliminate any yaw or roll freedom in the model. In this way with the frame pivoted at the tunnel floor and at the craft, it was possible to investigate the pitch performance of the system in a hover mode with low tunnel flow. Then as the tunnel speed was increased the craft was converted to a generation mode, all on both rotors. The tailplane incidence and the collective pitch on each rotor were manually controlled by a standard radio-control servo link. The servos can be clearly identified in Fig. 23.6. No cyclic pitch action was provided.

In summary, it is envisaged that a craft having twin, and sometime later having quadruple or more rotors, can generate electrical power at altitude with the rotors inclined at an adjustable angle to the on-coming wind. In general the rotor disks operate at an angle of about $\alpha_c = 40^\circ$. The wind then acts on the inclined rotors

producing lift, gyroplane-style, while simultaneously driving the rotors to generate electricity, windmill-style. The electricity so generated is conducted down the tether to a ground station.

It is also important to consider that the craft can also function as an elementary powered helicopter with electrical energy supplied from the ground, with the generators then functioning as motors. The craft can then ascend, descend or maintain altitude during any short wind lull aloft. A ground winch, which could reel the tether, would be used to retrieve the craft in an emergency. Obviously a single conducting tether would be preferable.

23.5 Atmospheric Craft

An atmospheric test vehicle was next designed and constructed. A picture of the craft close to auto-rotation is shown in Fig. 23.7. A full report on the design and

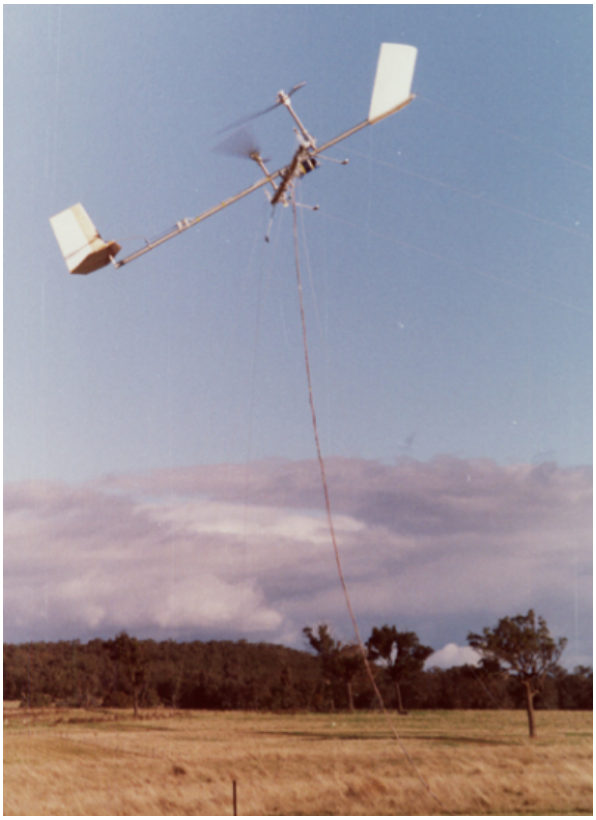

Fig. 23.7 The Gyromilll Mk2 was equipped with twin, single bladed, counterweighted rotors of solidity 2.2% and a diameter of 3.65 m. The total mass of the craft was 29 kg. Again no cyclic pitch capability was employed. Thus in hover and wind it was found necessary to use three parallel tethers to maintain craft attitude. These three tethers were used in all tests, but the craft was difficult to control particularly in low winds. Two tethers were attached near the rotor thrust lines while the third tether was attached well forward on the forward pointing boom

preliminary performance of this craft is given in reference [14]. The craft generated power at about 50 feet altitude for a short period, but in hindsight it was very difficult to control without the use of a then unobtainable modern gyro-stabilizing avionics. Next it was decided to use a four or more rotor system in order to have active attitude control by employing differential collective pitch action on at least four rotors without the use of cyclic action. The avoidance of cyclic action should greatly enhance the fatigue life, while making each rotor's control system almost identical to that of well-proven ground-based wind turbines.

23.6 Quad-Rotor System

This arrangement consists of four identical rotors in mutual counter-rotation. They can be mounted in a suitable airframe which is tethered by a single tether in the powerful and persistent winds aloft. The strength element of the electro-mechanical cable can be of the Kevlar family. This element is wound together with insulated aluminum, or possibly copper, conductors. For high-altitude operation a high-voltage, direct current (HVDC) system is preferred with transmission voltages of about 15 kV, or more. This amounts to about 3 volts per meter of operating altitude. It is acknowledged that conductor insulation could be an issue, but current advice is that these voltages are achievable in a twin-conductor, DC system. This high voltage is necessary if the tether weight is not to be excessive compared to the weight of the craft. This important weight issue will be discussed further below. The rated output per unit from these high-altitude, multiple-rotor systems is envisaged to be in the 3 to 30 MW range, making them useful for commercial electricity production. These generators at high altitude would avoid community concerns about the visual and noise intrusions usually associated with conventional ground-based wind turbines. Also there is a lesser of a bird-strike problem. Nevertheless, they would need to be placed in restricted airspace to avoid intrusion by other aircraft and to be located away from populated areas. While an array of these generators at altitude would be similar to conventional wind farms, in most instances the craft can be located much closer to the demand load centers than that of ground-based wind farms.

When operating as an electric generator the quadruple, or more rotors, are inclined at an adjustable and controllable angle to the on-coming wind. In general the rotors have disk incidence angles up to no more than $\alpha_c = 50^\circ$. The disk incidence is reduced in increasing wind conditions so as to hold the power output at its rated value without exceeding the safe tether load. This can be achieved while maintaining altitude and by varying the rotor's rotational speed, all without introducing excessive retreating blade incidences.

It can be shown that with all factors considered, the capacity (availability or generating) factor of these craft is far higher than that obtainable from the very best ground-based wind turbines. Reference [18] quotes capacity factors for high-altitude rotorcraft at between 71 and 90% for a number of US sites. Typical capacity factors for ground-based turbines are only about 30%. Therefore, it can be concluded

that high-altitude craft can be classed as base-load generators, if the above capacity factors were to be demonstrated.

Figure 23.8 shows a quad-rotorcraft with four identical rotors arranged with a forward pair of rotors ahead of a rearward pair. The rotors are in mutual counter-

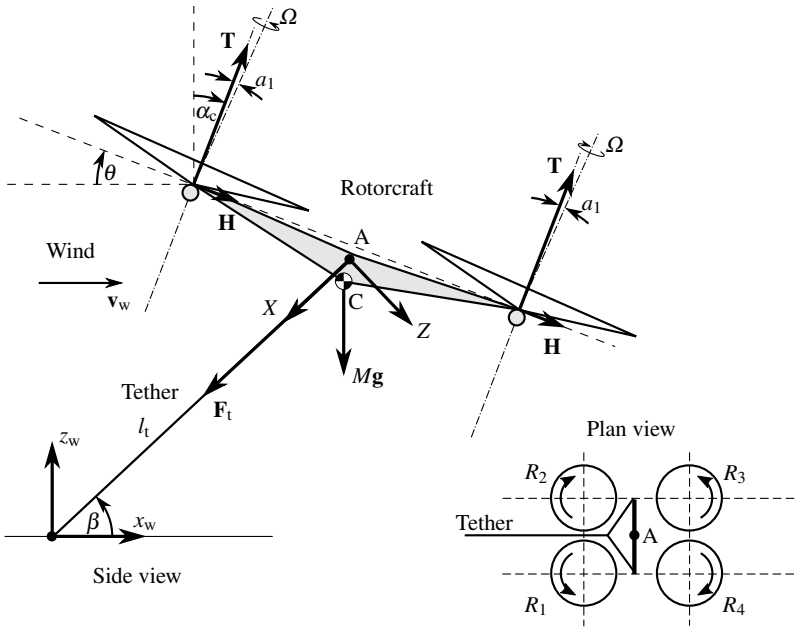

Fig. 23.8 Configuration of a typical quad-rotorcraft in side and plan view for the case of no cyclic pitch ($\theta = \alpha_c$), showing the wind reference frame (x_w, z_w) and the tether reference frame (X, Z)

rotation [16]. Thus each rotor rotates in an opposite direction to that of its two adjacent neighbours. With this particular arrangement the craft's pitch, roll and yaw can be controlled by the application of collective pitch changes to the rotors. No cyclic pitch action is necessary. This will help reduce construction costs and maintenance expenses. Variation of collective pitch thus changes the thrust developed by each rotor in a format described below using gyro-derived error signal data [13].

- Total craft thrust (i.e. craft altitude and power output) is controlled by collective pitch action on all rotors applied simultaneously by equal amounts.
- Roll control is by differential collective action between the port and starboard pair of rotors by an equal amount.
- Pitch control is by differential collective pitch action between the forward and rearward pair of rotors by an equal amount.
- Yaw control is through differential torque reaction. This by the application of differential collective pitch changes on pairs of opposite rotors by equal amounts.

It should be noted that there is a yaw control reversal at low wind speeds, so it is recommended that the differential collective action described above be used for hover and low wind speeds only. At wind speeds above the yaw reversal it is recommended a vertical stabilizer, namely a fin and rudder, be designed with sufficient control authority to enable the yaw control system described above to be disabled at higher wind speeds.

Tethered craft at high altitude have a further inherent advantage over ground-based wind turbines. This is their ability to reduce the effects of gust induced loads and torques. This is due to the flexibility of the tether cable which does not exist in the rigidly mounted ground-based equivalent. This flexibility arises from cable elasticity and from the change in cable shape under gust conditions. This inherent flexibility results in a very significant alleviation in the gust loads and torques applied to rotors, gearboxes etc. This alleviation is estimated to be more than an order of magnitude reduction. Further work is required on this matter.

23.7 Equilibrium Flight Performance of a Quad-Rotorcraft

In this section we will examine the equilibrium performance of a typical quad-rotorcraft in generating flight in reference to the configuration illustrated in Fig. 23.8. Various forms of rotor arrangements are conceivable, however, for simplicity of the analysis, a rectangular layout in plan view is assumed.

The rotorcraft is exposed to a steady wind of velocity v_w. The nose-up angle of the craft is denoted by θ, which is identical to the control axis angle α_c of the rotors because no cyclic pitch is used. The rotor's flapping angle a_1 is shown as the angle between the normal to the tip-path plane and the control axis. The total rotor thrust component along the control axis is $\mathbf{T}$ and normal to this axis is the component force $\mathbf{H}$. To account for the aerodynamic drag of the fuselage the additional force $\mathbf{D}_{fus}$ is added. Because at equilibrium flight conditions the rotorcraft is not moving the drag of the fuselage is aligned with the wind velocity.

A single, straight tether of length l_t is attached at point A to the craft on its plane of longitudinal symmetry. This attachment point is the origin of the tether reference frame which has its X- and Z-axes aligned with and normal to the tether. The gravitational force $M\mathbf{g}$ acts on the craft's center of mass which is denoted as point C. The points A and C may be coincident, but this is not a necessary requirement. The tether is assumed for simplicity to be massless, inextensible and with an infinitesimal diameter, at the present stage of this analysis. It is represented by a straight line. These simplifying assumptions for the tether are reasonable provided its length is around 300 m or less. However, for higher altitudes the analysis has been extended to include tether mass and the wind loads. The tether force $\mathbf{F}_t$ is aligned with the tether because of the straight-line assumption and the fact that the flexible tether can only transfer a tensile force.

A number of equilibrium studies have been made by Ho [6], Roberts [15] and Jabbarzadeh [8] for the twin and quad-rotor arrangements described above. These

used the classical rotor theory of Gessow and Crim [4], which is applicable to the current high disk incidence angles at high inflow conditions. It was assumed for simplicity in all these studies that all four rotors were in identical operation and each are in isolated air flows. Thus, aerodynamic interference between rotors was not taken into account, nor any aerodynamic interaction with the fuselage. The resulting equilibrium force polygon for the quad-rotor system is shown in Fig. 23.9.

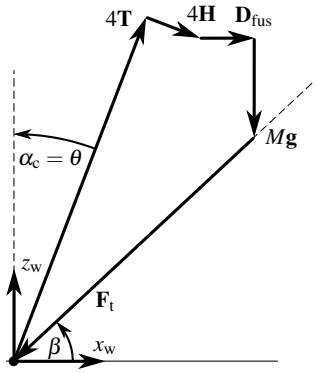

Fig. 23.9 Equilibrium force polygon for the quad-rotorcraft involving the total rotor thrust 4**T** and total H-force 4**H**, the tether force $\mathbf{F}_t$, the craft gravitational force $M\mathbf{g}$ and the aerodynamic drag force on the fuselage $\mathbf{D}_{\text{fus}}$

The power coefficient C_p and aerodynamic lift coefficient C_L of an individual rotor are shown in Figs. 23.10 and 23.11, respectively. It should be noted that C_p is normalized using the wind velocity, as in wind turbine practice, instead of normalized using the rotor tip speed, as in helicopter practice. Note that a positive sign of

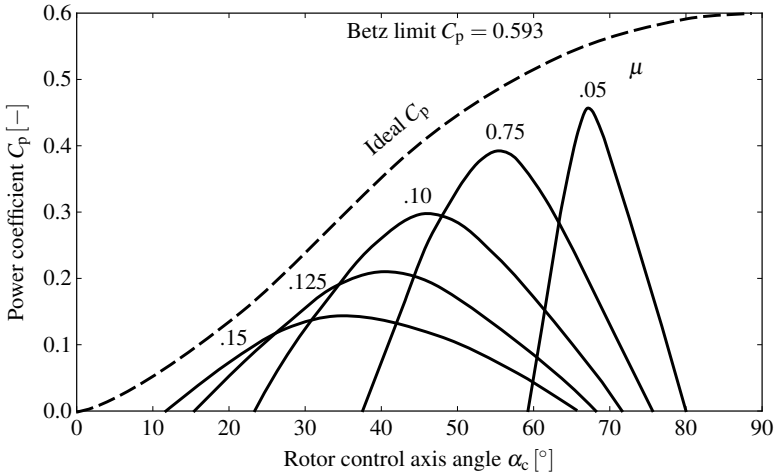

Fig. 23.10 Power coefficient C_p of a single rotor as function of the rotor control axis angle α_c, for various values of the tip speed ratio μ

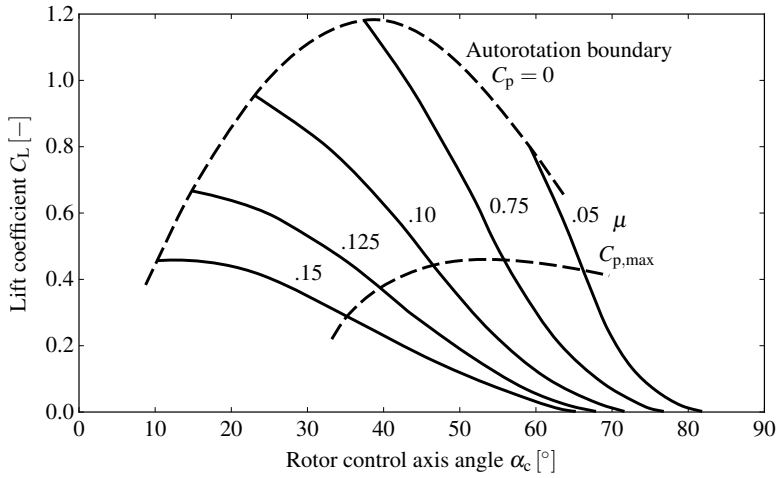

Fig. 23.11 Aerodynamic lift coefficient C_L of a single rotor as function of the rotor control axis angle α_c, for various values of the tip speed ratio μ

C_p implies a power output, this being opposite to that used in helicopter theory. The lift coefficient is normalized using the wind velocity. The tip speed ratio used is as defined in helicopter theory. Both figures were calculated by Jabbarzadeh [8] using a rotor solidity $\sigma = 0.05$, linear twist of the blades $\theta_1 = +8^\circ$, Lock number $\gamma = 10$, tip loss factor $B = 0.97$ and operating all rotors at a retreating blade incidence limit, as normally defined, with a value 13°.

The dashed curve in Fig. 23.10 represents the ideal, maximum power output, that could be obtained for zero profile drag of the rotor blades. Hence the bell-shaped curves derived from Gessow and Crim [4], incorporating profile drag effects, will always lie below the ideal, dashed curve. The curves are terminated at $C_p = 0$ which represents autorotation conditions, where no power is being developed or supplied. The favored autorotation condition, to be discussed below, is one of the left-hand, abscissa crossings of the bell-shaped curves. Only the left-hand, zero crossings will be considered in what follows.

In Fig. 23.11 the C_L-curves all terminate on the uppermost dashed curve. At this limit the rotors are in autorotation, with the values of lift coefficient at their individual maxima and with the power output at zero. It can be seen that the maximum lift coefficient occurs at $\alpha_c \approx 40^\circ$ and $\mu \approx 0.075$. In addition, it is important to note the following. The maxima of the bell-shaped curves shown in Fig. 23.10 are shown as a locus-line drawn as the lowermost dotted curve of Fig. 23.11. In other words, equilibrium operations are best performed anywhere between the two dotted curves shown on Fig. 23.11. The closer operations are made to the lower dotted curve the greater will be the power output, but the craft's available thrust will reduce as operations approach this lower dotted curve. Operations are possible below the abscissa of Fig. 23.10, but power must be supplied to the system to develop sustainable lift.

23.8 Best Autorotation Conditions

Autorotation relates physically to the flight condition where the system is on the point of collapse due to insufficient wind speed being available to support the craft and its tether without any input of power to the rotors. The left-hand side crossing of the bell-shaped curves with the ordinate axis in Fig. 23.10 implies that no power is being produced and all the wind's kinetic energy is being used to generate lift. A left-hand cutting at a lesser control axis angle than on the right-hand crossing is preferred, because this condition is more favorable from a tether viewpoint. This means that a lower nose-up attitude of the craft gives a tether closer to the vertical with a resulting lower tether length. The question then arises as to which of the left-hand crossings is most favorable to give the lowest wind speed to keep the system aloft in the critical autorotation condition? This minimum wind speed can be determined by considering vertical force equilibrium in Fig. 23.9. It can be shown that the ratio of the craft's weight disk loading to the free stream dynamic pressure,

$$\frac{\frac{Mg}{4\pi R^2}}{\frac{1}{2}\rho v_{\mathrm{w}}^2} = C_{\mathrm{L}}[1-\tan(\alpha_{\mathrm{c}}+a_1)\tan\beta], \tag{23.2}$$

is the important relevant parameter, with α_{c} denoting the rotor control axis angle and a_1 denoting the rotor backward tilt angle. The left-hand side of this equation has to be organized to be at its maximum value in order to achieve the minimum wind speed for a given craft weight disk loading.

The variation of the weight disk loading to dynamic pressure ratio is shown in Fig. 23.12. A reasonable value for β may be, say, 35°. For this particular case, the

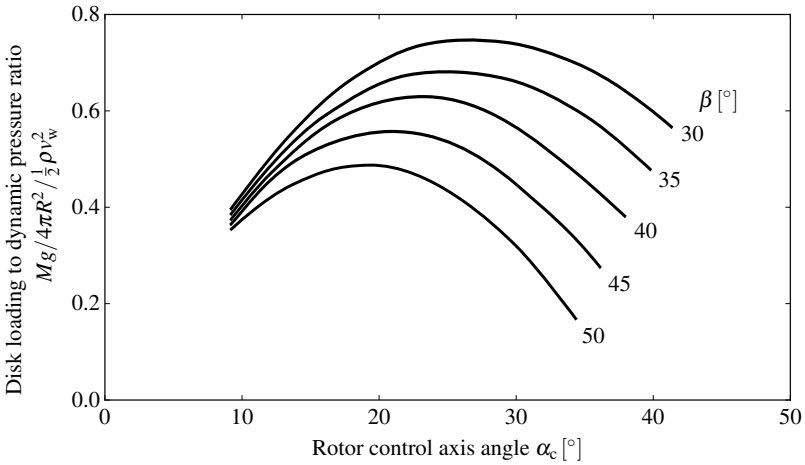

Fig. 23.12 Weight disk loading to dynamic pressure ratio as a function of rotor control axis angle α_{c}, for various values of the elevation angle β

best autorotation conditions can be read-off Fig. 23.12 to give a control axis angle of 25° at a corresponding tip speed ratio of 0.093. An extremely important conclusion can now be drawn from Fig. 23.12.

If a high-altitude craft, with 5% solidity, were to have a straight, massless tether arranged at an angle of, say, 35° to the horizontal, then for the craft to stay aloft the craft's weight disk loading to dynamic pressure ratio, as read from Fig. 23.10, cannot exceed 0.69. If we wish to fly it in autorotation at 15,000 feet in, say, a 10 m/s wind, then the weight disk loading must be at or less than 0.69×38.5 Pa, or 0.553 lb/ft^2. In other words, the craft's weight disk loading must be low by rotorcraft standards, and it must not exceed 0.553 lb/ft^2 to achieve an autorotation speed of 10 m/s at the nominated 35° cable angle.

In making the above statement it is realized that the tether has been assumed to be weightless. Of course, a change in the autorotation speed quoted above will be in proportion to the square root of any change in the weight disk loading, all other factors remaining the same. It should be noted that the disk loading is based on the weight Mg of the craft. Because the tether force acting on the craft is much larger than the gravitational force, it means that the craft's disk loading based on weight should be much less than that used on untethered rotorcraft.

23.9 Consideration of Tether Weight

We will now formally introduce tether weight to calculate the operating envelope for an example craft. Wind loads on the tether and the craft's fuselage drag will be here neglected for simplicity. However Roberts [11] has available full computer codes which do include these two effects. Put simply, it is considered here to be more explicit if we consider the cable mass without the imprecision of the actual tether's wind profile, along with the uncertainty of the craft's drag coefficient.

A preliminary system analysis, to be used for a demonstration of the analysis technique, can now be developed assuming that the tether is of uniform mass per unit length. Thus the tether forms a catenary attached at the point A shown in Fig. 23.8. Thus from point A in the craft, the tether drapes down to an anchor point on the ground.

Consider, for the demonstration, a quad-rotorcraft with rotors of radius $R = 12.35$ m (≈ 80 ft) with a solidity of $\sigma = 0.05$. In this example we use a NACA 0012 blade section with the conventional blade and rotor parameters. Four basic modes of operation can be defined:

Mode A: Rated power output in any wind above the rated speed.
Mode B: Rated power at rated wind speed.
Mode C: Part power output in light winds.

Mode D: Autorotation at the minimum sustainable wind speed.

Next, assume the craft is configured to give a rated power output of 3.1 MW at an altitude of 15,000 feet. A tether weight of 460 kg/km has been assumed, using Kevlar as the tensile member and incorporating twin, insulated aluminum conductors. A combined electrical efficiency for the generator and tether transmission has been taken as 90%. The result would be a tether about 15 mm in diameter with the Kevlar stressed to an adequate and safe level.

A central aspect of the design would be operation in mode B. Here the craft is best at a nose-up attitude of 47° at a wind speed of 25.8 m/s. It then develops the rated power of 3.1 MW. This produces a tether tension of 300 kN. At any wind speed greater than 25.8 m/s, such as in mode A, the system should not exceed its peak rating both electrically and structurally. Thus the craft maximum power output and its maximum tether tension have been frozen at the above values, never to be exceeded.

The craft weight has been estimated to be 3135 kg. This gives the weight disk loading for the vehicle of 0.333 lb/ft^2 (c.f. this value with the 0.553 lb/ft^2 statement in the previous section). In this example craft, the rated output power loading is 150 W/ft^2.

The system characteristics for the different modes of operation are shown in Table 23.1. Mode C is shown for part-power operation in a wind of 18.3 m/s, while

	Operating Mode			
Description	A	B	C	D
Electrical power output, MW	3.13	3.13	1.26	0
Altitude of craft, km	4.57	4.57	4.57	4.57
Incidence of rotors, deg	27.4	47.0	49.4	26.0
Wind speed, m/s	36.6	25.8	18.3	10.2
Total craft mass, kg	3135	3135	3135	3135
Mass of tether, kg	2592	3846	4402	4620
Maximum tether tension, kN	300	300	232	61
h/y at or above wind speed	570	2280	4330	6950

Table 23.1 System characteristics for different modes of operation

mode D is autorotation at the lowest sustainable wind of 10.2 m/s. The hours of operation at or above the wind speeds for each mode have been extracted from the Weibull charts for Albany in the USA [10], or for Moree in Australia [8] at an altitude of 15,000 feet. These two sites are almost identical in their wind probability data.

The above results can be used to construct a power-duration curve for the system. This gives an annual capacity factor of about 50% with a total annual energy output of 13.3 GWh. The percentage of time per annum that the craft would need to be landed is 20.3%.

Finally, it is interesting to calculate side elevations of the craft and its tether in the modes A through D. These are given in Fig. 23.13, again assuming no aerodynamic loading on the tether, but solely taking into account the effect of gravity.

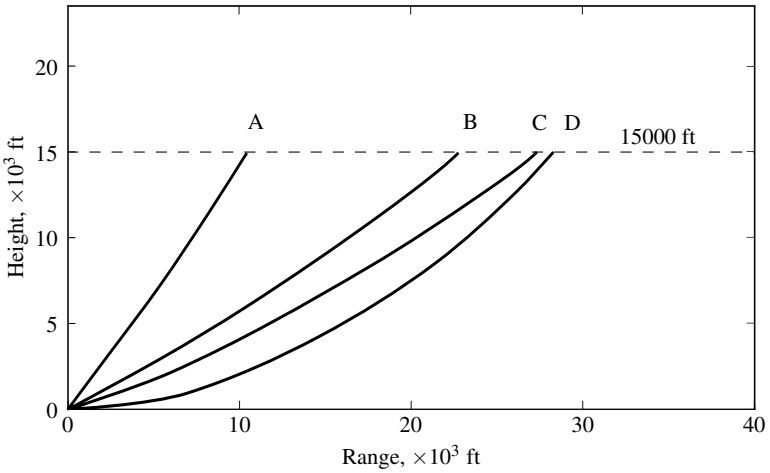

Fig. 23.13 Side elevations of the craft and its tether in the modes A through D

23.10 Quad-Rotorcraft Stability and Control

It is well-known that rotorcraft are inherently unstable if left uncontrolled. A control strategy is therefore essential for the operation of the system, stabilizing pitch, roll and yaw, with pitch being the important variable.

We will discuss longitudinal and lateral stability assuming for simplicity that the tether is straight, massless and inextensible, as shown in Fig. 23.8. This assumption is reasonable, provided the tethering cable is relative light and short in length, namely about 100 m. If the tether is straight and inextensible, the craft's longitudinal motions will be solely pitch and heave, with the point A in Fig. 23.8 moving only in tangential direction (Z-axis), perpendicular to the tether. Motion in the radial diraction (X-axis) is not possible. Lateral motion (Y-axis) can also be examined under the same assumptions. On the above basis the stability and control can be simply examined without the introduction of tether dynamics. Of course the tether could be included, but considerably more complication would be required.

Ho [6], Strudwicke [20] and Roberts [15] have studied the longitudinal stability of a twin-rotorcraft, while Roberts [15] has extensively studied both the longitudinal and lateral stability of the quad-rotor system. For the quad-rotor system, under the assumptions given above, the coupled pitch θ and z-motions from an equilibrium

position of the rotorcraft are coupled and unstable, when the craft's controls are fixed. However, the system can be easily stabilized using a proportional and damped (PD) controller using differential collective pitch action on the rotors, as described in Sect. 23.6. This form of controller uses as its input only the error-signal between the actual and desired pitch angles of the craft. This error-signal is used to action the four rotors' collective pitch angle, differentially from their equilibrium positions, by an equal positive or negative amount of magnitude $\Delta\theta_0$.

The equations of motion for small perturbations of the rotorcraft from its equilibrium configuration, namely its position, pitch angle (nose-up angle) θ and rotor collective pitch θ_0, can be studied by firstly setting-up the relevant rotor force derivatives for disturbed flight from the equilibrium conditions. Begin by calculating the force derivatives X_u, Z_u, X_w, Z_w, X_q, Z_q, X_θ and Z_θ in the wind reference frame following standard texts, such as Bramwell [2]. It should be noted that Bramwell's formulation uses x- and z-axes in opposite direction to the x_w- and z_w-axes of the wind reference frame shown in Figs. 23.8 and 23.9. In addition, the control force derivatives, $T_{\theta,0}$ and $H_{\theta,0}$, can be computed.

The next step in the calculation schedule is to transform the rotor force derivatives to the tether reference frame, using the equations of Seckel [19, p. 463]. For the purpose of this perturbation analysis the tether reference frame is spacially locked to its equilibrium state. With reference to Fig. 23.8 this transformation from wind to tether reference frame is a counter-clockwise rotation with an angle $180^\circ + \beta$. This transforms all the force derivatives into perturbations associated with displacements and motions measured in the tether reference frame (X, Z). The reason for this transformation, as mentioned above, is that any x-perturbation is eliminated, if the tether is straight and inextensible. Therefore, the current analysis reduces from a system having three degrees of freedom to one of only two degrees, namely simply studied with z- and θ-perturbations.

The next step in the rotor calculations is to sum the derivatives for all of the four rotors to calculate the forces in total on the vehicle. Also in addition, calculate the moment derivatives knowing the physical size and configuration of the rotors in the craft's airframe. Care should be taken to express all moment derivatives as moments about the craft's center of mass. Referring to Fig. 23.8 the center of mass C is generally not coincident with the attachment point A. This latter point is important when compiling the rotorcraft's equations of motion for small perturbations from the equilibrium position. The equations of motion can now be written as

$$\mathbf{M}\begin{bmatrix}\ddot{z}\\ \ddot{\theta}\end{bmatrix} + \mathbf{D}\begin{bmatrix}\dot{z}\\ \dot{\theta}\end{bmatrix} + \mathbf{K}\begin{bmatrix}z\\ \theta\end{bmatrix} = \begin{bmatrix}\delta\\ \eta\end{bmatrix}\Delta\theta_0, \tag{23.3}$$

$$\theta_{0;1,2} = \bar{\theta}_{0;1,2} + \Delta\theta_0, \tag{23.4}$$

$$\theta_{0;3,4} = \bar{\theta}_{0;3,4} - \Delta\theta_0, \tag{23.5}$$

where $\mathbf{M}$ represents the mass matrix, $\mathbf{D}$ the damping matrix and $\mathbf{K}$ the stiffness matrix. This matrix equation represents a double-output, single-input control system. Such a system is often called a "follower system", where in the present case the displacement z simply follows the value of θ. The right-hand side column matrix shows

the force and moment control derivatives, where the craft's control derivatives are the coefficients δ and η. Now because we have chosen the rotor arrangement as in Fig. 23.8 and having incorporated the differential collective pitch action, as defined in Eqs. (23.4) and (23.5), it follows that $\delta = 0$. However, the η-term, being the control moment, has a finite value, which in effect controls the craft's pitch attitude.

The matrices on the left-hand side of Eq. (23.3) can be derived using the appropriate derivatives involving the craft's position, pitch angle, velocity, pitch rate and the acceleration of point A. The **D**-matrix is determined using the above rotor derivatives, the **M**-matrix by using the mass and moment of inertia of the craft noting that the point A may not be coincident with C, while the **K**-matrix is essentially determined by the tether tension and the perturbation of point A in the Z-direction.

In Eqs. (23.4) and (23.5) a collective pitch change, $\Delta\theta_0$, is applied equally to the R_1 and R_2 rotors, while an opposite change of the same magnitude is applied to rotors R_3 and R_4. After considerable work it has been found that for a craft of almost any size, it can be stabilized by the application in a PD controller with a proportional gain of about 0.1 to 0.2° of collective pitch change per degree of error in the craft's pitch angle. This value of controller gain is strongly dependent on the distance between the fore and aft rotor mounting in the fuselage. A damping term in the controller could also be useful.

A similar philosophy for the control of the roll and yaw should lead to a favorable outcome. However, the control of yaw is subject to the yaw reversal effect discussed in Sect. 23.6. Differential collective pitch for yaw control, in or near hover, has the above mentioned control reversal. To counter this effect a vertical stabilizer (vertical fin) and rudder should be used for yaw control when generating power in windy conditions. In the latter condition yaw control by differential collective would be disabled.

23.11 Conclusions

It has been shown from atmospheric data that that the wind speed and wind power increases with increasing altitude, up to the tropopause level. In order to harness this enormous energy a quad-rotorcraft has been proposed and analyzed.

Graphs are shown in Figs. 23.10 and 23.11 for the power and lift coefficients as functions of control axis angle, parametrized by the tip speed ratio, for a rotor solidity of 5%. Other solidities would give similarly shaped graphs. In Fig. 23.11 it can be seen that realistic operations can occur anywhere between the two dashed curves therein. Fig. 23.12 shows for various tether elevation angles how different weight disk loadings to dynamic pressure ratios are necessary in order to maintain operations at the limiting autorotation condition.

For demonstration purposes the above theory has been applied to a sample craft operating at an altitude of 15,000 feet. This altitude has been chosen simply because it is well established that an electro-mechanical tether to this altitude is feasible. These altitudes have been used twenty four hours a day, seven days a week, for

border protection duties in the USA for some years. In this situation the tether is attached to and restrains the tethered balloon. Next a 3.15 MW quad-rotor system at 15,000 feet has been chosen to demonstrate that the technology is feasible, but this example is not proposed as the optimal altitude for any construction. This craft has been shown to give a generating capacity factor of 50%. It is suggested here that operations at somewhat higher altitudes, namely 20,000 to 25,000 feet could give significant power outputs at capacity factors of between 70 and 80%.

The chapter concludes by examining the stability and control of a quad-rotorcraft. This theory is applicable at any trim rotor incidence and rotor tip speed ratio. It is shown that differential collective pitch action on the rotors can control the rotorcraft in pitch, roll and yaw. However, the yaw control theory confirms that a control inversion occurs early in the craft's operating range. To avoid yaw difficulties, differential collective pitch action is proposed only for low wind speeds. At higher wind speeds a conventional vertical stabilizer and rudder is proposed, with the collective pitch action disabled.

Editors note After the compilation of this chapter a very interesting contemporary analysis of the gyrocopter-type airborne wind energy system has been published by Rancourt et al. [11].

References

1. Atkinson, J. D. et al.: The Use of Australian Upper Wind Data in the Design of an Electrical Generating Platform. Charles Kolling Research Laboratory Technical Note TN D-17, 1–19 (1979)
2. Bramwell, A. R. S.: Helicopter Dynamics. Edward Arnold (Publishers) Ltd., London, UK (1976)
3. Fletcher, C. A. J., Roberts, B. W.: Electricity generation from jet-stream winds. Journal of Energy **3**(4), 241–249 (1979). doi: 10.2514/3.48003
4. Gessow, A., Crim, A. D.: An extension of lifting rotor theory to cover operation at large angles of attack and high inflow conditions. Technical Report NACA TN-2665, Langley Aeronautical Laboratory, Langley Field, VA, US, Apr 1952. http://naca.central.cranfield.ac.uk/reports/1952/naca-tn-2665.pdf
5. Gessow, A., Myers Jr., G. C.: Aerodynamics of the Helicopter. Macmillan Co., New York, NY (1952)
6. Ho, R. H. S.: Lateral Stability and Control of a Flying Wind Generator. M. E. (Res) Thesis. M.Sc.Thesis, University of Sydney, Nov 1992. http://hdl.handle.net/2123/2609
7. Hoffert, M. I., Caldeira, K., Jain, A. K. et al.: Energy Implications of Future Stabilization of Atmospheric CO_2 Content. Nature **395**, 881–884 (1998). doi: 10.1038/27638
8. Jabbarzadeh Khoei, A.: Optimum Twist for Windmill Operation of a Tethered Helicopter. M. E. Studies Thesis. M.Sc.Thesis, University of Sydney, Aug 1993. http://hdl.handle.net/2123/2608
9. Manalis, M. S.: Airborne Windmills and Communication Aerostats. Journal of Aircraft **13**(7), 543–544 (1976). doi: 10.2514/3.58686
10. O'Doherty, R. J., Roberts, B. W.: The Application of U.S. Upper Wind Data in One Design of Tethered Wind Energy Systems. SERI/TR-211-1400, Solar Energy Research Institute, Golden, CO, USA, Feb 1982. doi: 10.2172/5390948

11. Rancourt, D., Bolduc-Teasdale, F., Demers Bouchard, E., Anderson, M. J., Mavris, D. N.: Design space exploration of gyrocopter-type airborne wind turbines. Wind Energy **19**, 895–909 (2016). doi: 10.1002/we.1873
12. Roberts, B. W.: Quad-Rotorcraft to Harness High Altitude Wind Energy. In: Schmehl, R. (ed.). Book of Abstracts of the International Airborne Wind Energy Conference 2015, pp. 84–85, Delft, The Netherlands, 15–16 June 2015. doi: 10.4233/uuid:7df59b79-2c6b-4e30-bd58-8454f493bb09. Presentation video recording available from: https://collegerama.tudelft.nl/Mediasite/Play/102d7cb3437542acbf4078bac1e853eb1d
13. Roberts, B. W.: Control System for A Windmill Kite. Australian Patent 2009238195, Apr 2009
14. Roberts, B. W.: Design and Preliminary Performance of the Gyromill Mk2. End of grant report 380, Department of Resources and Energy, Canberra, Australia, Oct 1984. http://nla.gov.au/nla.cat-vn2242481
15. Roberts, B. W.: Private papers
16. Roberts, B. W.: Windmill Kite. US Patent 6,781,254, Aug 2004
17. Roberts, B. W., Blackler, J.: Various Systems for Generation of Electricity Using Upper Atmospheric Winds. In: Proceedings of the 2nd Wind Energy Innovation Systems Conference, pp. 67–80, Solar Energy Research Institute, Colorado Springs, CO, USA, 3–5 Dec 1980
18. Roberts, B. W., Shepard, D. H., Caldeira, K., Cannon, M. E., Eccles, D. G., Grenier, A. J., Freidin, J. F.: Harnessing High-Altitude Wind Power. IEEE Transactions on Energy Conversion **22**(1), 136–144 (2007). doi: 10.1109/TEC.2006.889603
19. Sechel, E.: Stability and Control of Airplanes and Helicopters. Academic Press, New York (1964)
20. Strudwicke, C. D.: A Control System for a Power Generating Tethered Rotorcraft. M. E. (Res) Thesis. M.Sc.Thesis, University of Sydney, Nov 1995. http://hdl.handle.net/2123/4993